

Cite this: *New J. Chem.*, 2011, **35**, 1640–1648

www.rsc.org/njc

Synthesis and stability of 2-tetrazenium salts†

Carles Miró Sabaté* and Henri Delalu

Received (in Montpellier, France) 25th March 2011, Accepted 10th May 2011

DOI: 10.1039/c1nj20278b

The geometry and electronic structure of (*E*)-N₄Me₄ (**1**) and the (*E*)-N₄Me₄H⁺ and the (*E*)-N₄Me₅⁺ cations was examined by a DFT approach. By using the B3LYP/6-31+G(d,p) model we showed that the terminal nitrogen atoms in **1** are strongly basic, as evidenced by their highly negative NBO charges in comparison to the azo nitrogen atoms. Interestingly, protonation of **1** to form the (*E*)-N₄Me₄H⁺ cation does not result in significant changes in the NBO charges of the protonated nitrogen atom, which is in contrast with classical views that describe tetracoordinated nitrogen atoms as being positively charged. Insight into the thermal stability of salts of the (*E*)-N₄Me₄H⁺ and the (*E*)-N₄Me₅⁺ cations was gained experimentally by DSC measurements of two salts of the (*E*)-N₄Me₄H⁺ cation, namely with chloride (**2**) and picrate (**3**) anions and the iodide salt of the (*E*)-N₄Me₅⁺ cation (**4**), which were synthesized by protonation of **1** with hydrochloric (**2**) and picric (**3**) acids and by methylation of **1** with methyl iodide (**4**), respectively. Compounds **2–4** were characterized by analytical (elemental analysis and mass spectrometry) and spectroscopic (¹H/¹³C NMR, IR/Raman and UV spectroscopies) methods. Protonation and methylation of **1** to form the (*E*)-N₄Me₄H⁺ (compounds **2** and **3**) and (*E*)-N₄Me₅⁺ (compound **4**) cations, respectively, appears to occur at the terminal nitrogen atoms, in keeping with the results of the NBO analysis and the higher stabilization energy of the conformations with a protonated/methylated terminal nitrogen atom. The geometry optimization by the B3LYP/6-31+G(d,p) method points at very weak N3–N4 bonds (N4 = protonated/methylated nitrogen atom), which explains the formation of dimethylammonium picrate in the thermal decomposition of picrate salt **3** and suggests that dialkylaminium radicals (R₂N⁺•) are involved in the decomposition pathway.

Introduction

Interest in the synthesis and analysis of the energetic properties of HEDMs = high-energy density materials continues.^{1–7} Classical energetic materials such as TNT = trinitrotoluene or RDX = cyclotrimethylenetrinitramine derive their energy from the oxidation of their carbon backbones,^{8,9} in contrast to N–N compounds, which owe their high energies to their positive heats of formation.^{10,11} Unfortunately, many of these materials are highly sensitive and accidents have occurred in the past. Other compounds such as hydrazine and its derivatives, *e.g.*, MMH = monomethylhydrazine or UDMH = unsymmetrical dimethylhydrazine form hypergolic mixtures with oxidizers such as NTO = nitrogen tetroxide or LOX = liquid oxygen and are, therefore, widely used in hypergolic rocket fuels as a

bipropellant component. Unfortunately, hydrazine and its derivatives have high vapour pressures and are known to be toxic and carcinogenic. Additionally, high purity hydrazines might form explosive mixtures with air.¹² In this context, salt formation is known to stabilize a material¹³ and, additionally, ionic materials tend to display lower vapour pressures and higher densities (related to the performance of the compound) than their atomically similar non-ionic derivatives.¹⁴

Recently, 2-tetrazenes (Fig. 1) have emerged as a class of energetic materials with good chemical and thermal stability and lower toxicity than commonly used compounds.¹⁵ 2-Tetrazenes are isoelectronic with the butadiene dianion, *i.e.*, they are electron-rich compounds with several lone pairs. For this reason they are involved in both intra- and extra-molecular hydrogen-bonding.¹⁶ The electron-rich character give them also a high intrinsic basicity (*e.g.*, p*K*_b (N₄Et₄) = 5.12),¹⁷ which increases with the larger the size of the substituent. The simplest

Laboratoire Hydrazines et Composés Énergétiques Polyazotés,
Université Claude Bernard Lyon 1, Bâtiment Berthollet, 3^e étage,
22, avenue Gaston Berger, 69622 Villeurbanne, France.

E-mail: carlos.miro-sabate@univ-lyon1.fr; Fax: +33-472-431-291

† Electronic supplementary information (ESI) available: Calculated IR/Raman frequencies and Mulliken charges for (*E*)-N₄Me₄ (**1**) and the N₄Me₄H⁺ and the N₄Me₅⁺ cations and hydrogen-bonding and graph-set tables for dimethylammonium picrate. See DOI: 10.1039/c1nj20278b

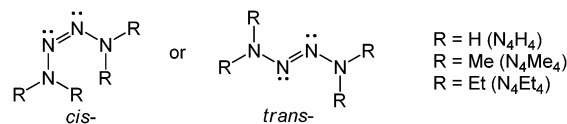


Fig. 1 Formula structures of *cis*- and *trans*-2-tetrazenes.

2-tetrazene possible, *i.e.*, N_4H_4 , ($R = H$) was synthesized as the *trans*- form by Wiberg and coworkers in 1975 over a four steps procedure starting from hydrazine.¹⁸ Unfortunately, this highly energetic compound is thermally labile and crystals of pure N_4H_4 might decompose explosively forming nitrogen gas, hydrazine and ammonium azide, even when stored at 0 °C. Additionally, salts based on the 2-tetrazenium cation, *i.e.*, $N_4H_5^+$, decompose at temperatures above *ca.* -20 °C forming ammonium salts and hydrazoic acid.¹⁹ The simplest 2-tetrazene known, which is stable at room conditions is the methyl derivative (*E*)- N_4Me_4 ($R = Me$) and much work has been carried out concerning the synthesis of the latter compound by the oxidation reaction of UDMH.^{15c,17,20–27}

Due to the interesting electronic properties of 2-tetrazenes and their potential for energetic applications, we became interested in studying the reaction of (*E*)- N_4Me_4 with hydrochloric and picric acids as well as with methyl iodide and the thermal stability of the resulting products.

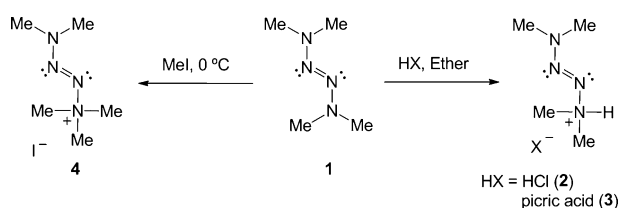
Results and discussion

Synthesis and stability

Oxidation of 1,1-dimethylhydrazine using mercury oxide in ether according to the method of Madginski and coworkers²³ afforded (*E*)- N_4Me_4 (**1**) as a pale yellow liquid. **1** was subsequently reacted with an equivalent amount of hydrochloric and picric acids to form the (*E*)- $N_4Me_4H^+$ cation as its chloride (**2**) and picrate (**3**) salts, which separated in high purity and yield from the ether reaction mixture. Additionally, **1** was reacted with an equivalent amount of methyl iodide in the cold and in the absence of solvent to form the iodide salt of the (*E*)- $N_4Me_5^+$ cation (**4**), which separated out of the reaction mixture (Scheme 1).

Compounds **2** and **4** were obtained as white powders, whereas the picrate salt **3** is a bright yellow solid. Both salts of the (*E*)- $N_4Me_4H^+$ cation (**2** and **3**) and that of the (*E*)- $N_4Me_5^+$ cation (**4**) are readily soluble in polar solvents such as water, DMSO or ethanol and insoluble in apolar solvent such as cyclohexane. In solvents like wet ether or toluene, suspensions of compound **3** turn yellow, possibly because of the formation of picric acid, which is soluble in these solvents. A similar behaviour is observed for **2** with the formation of hydrochloric acid. When dissolved in DMSO, compounds **3** and **4** give strong gas evolution. In water, **3** seems to have relatively good stability, however, when aqueous solutions of the compound are warmed, crystals of dimethylammonium picrate can be obtained (see discussion below).

In the solid state and in the absence of moisture, compound **2** decomposes within hours at room temperature, whereas the



Scheme 1 Protonation and alkylation of N_4Me_4 (**1**) to form the $N_4Me_4H^+$ and $N_4Me_5^+$ cations.

iodide salt **4** decomposes within a few days and the picrate salt **3** is stable for several weeks, slowly decomposing to form picric acid and **1**. In the refrigerator, compounds **3** and **4** can be stored for (at least) several weeks or even months, while **2** decomposes after a few days. In the freezer at *ca.* -20 °C, none of the three salts **2–4** showed appreciable decomposition after several months. When the solids are left standing in air, **4** decomposes within minutes into a reddish powder, *i.e.*, iodine formation, while **2** turns yellow and finally into a brown sticky mass with UV (H_2O) maxima at 242 nm, characteristic of (*E*)- N_4Me_4 (**1**). When the (*E*)- $N_4Me_4H^+$ salts (**2** and **3**) are overlaid with ether and left to stand for several hours (**2**) or days (**3**) in a closed vial and then the ether phase is analyzed by GC-MS, a signal at 2.01 min²⁸ with $m/z = 116.1$ is observed, which can be attributed to (*E*)- N_4Me_4 (**1**).

The thermal lability of compounds **2–4** is in keeping with the differential scanning calorimetry (DSC) results. Whereas (*E*)- N_4Me_4 (**1**) is stable up to its boiling point (*ca.* 130 °C), the chloride salt **2** decomposes already at *ca.* 57 °C and compound **3**, with the generally more thermally robust picrate anion,^{29,30} is stable up to *ca.* 72 °C. The above mentioned observations are also in agreement with the lower decomposition point of iodide **4**, which shows a sharp exotherm in the DSC measurements at *ca.* 52 °C (explosive decomposition!). All these results are in keeping with previous studies indicating that tetraaryl 2-tetrazenes start to decompose at *ca.* 40 °C.³¹ The low decomposition points of these compounds would limit their application in the field of energetic materials, however, the chloride salt **2** and the iodide salt **4** are expected to be useful intermediates for the synthesis of compounds with higher thermal stabilities that might be of energetic interest.

The UV spectra of the salts of the (*E*)- $N_4Me_4H^+$ cation (**2** and **3**) were measured in distilled water. We omitted the measurement for the salt of the (*E*)- $N_4Me_5^+$ cation (**4**) due to the strong gas evolution observed in this solvent, which lead to unreliable results. Salts **2** and **3** show one single maxima at 239 ($\epsilon = 7904 \text{ L mol}^{-1} \text{ cm}^{-1}$) and 245 ($\epsilon = 20520 \text{ L mol}^{-1} \text{ cm}^{-1}$) nm, respectively. By comparison, we measured (*E*)- N_4Me_4 (**1**) to give a single maxima at 242 ($\epsilon = 7640 \text{ L mol}^{-1} \text{ cm}^{-1}$), although depending on the solvent and/or concentration one peak at 277 nm with a shoulder at 250 nm might be observed. This effect has been attributed to the tendency of 2-tetrazenes to form protonated species in acidic solvents.¹⁷

Spectroscopic discussion

In order to facilitate the assignment of the signals observed in the infrared (IR) and Raman (Ra) spectra of (*E*)- N_4Me_4 (**1**) and the salts of the (*E*)- $N_4Me_4H^+$ (**2** and **3**) and (*E*)- $N_4Me_5^+$ (**4**) cations, we used DFT calculations (B3LYP/6-311+G(d,p)) to calculate the expected (gas phase) vibrational frequencies of (*E*)- N_4Me_4 (**1**) and the (*E*)- $N_4Me_4H^+$ and (*E*)- $N_4Me_5^+$ cations (see Experimental section for Computational details). Tables 1–3 of the ESI† show a summary of the computed frequencies (scaled and unscaled) with infrared intensities and Raman activities, comparison with the experimental results and tentative assignment of the vibrational bands for all three species.

The computed frequencies for compounds **1–4** are in relatively good agreement with the experimental values. The most important band observed in the vibrational spectra of compounds **1–4** is the N2–N3 azo bridge stretch, which is observed at IR/Ra frequencies of 1469/1473 cm^{-1} (**1**), 1490/Raman inactive cm^{-1} (averaged value for **2** and **3**) and 1480/1475 cm^{-1} (**4**). The stretching vibrations of the methyl groups C–H are observed in the range between 2960 and 3090 cm^{-1} (asymmetric C–H stretch) and between 2820 and 2885 cm^{-1} (symmetric C–H stretch) for compound **1**, between 2955 and 3020 cm^{-1} (asymmetric C–H stretch) and *ca.* 2920 cm^{-1} (symmetric C–H stretch) for salts **2** and **3** and between 3010 and 3070 cm^{-1} (asymmetric C–H stretch) and between 2840 and 2945 cm^{-1} (symmetric C–H stretch) for the iodide derivative **4**. Below these wave numbers in-plane bending vibrations of the methyl groups C–H are found, which go from 1440 to 1475 cm^{-1} (**1**), at *ca.* 1430 cm^{-1} (**2** and **3**) and from 1405 to 1480 cm^{-1} (**4**). At lower frequencies, the dominant vibrations are the stretching modes of the different C–N and N–N bonds present in the “N₄Me₄” moiety (“N₄Me₅” moiety for salt **4**) of compounds **1–4**. These vibrations extend up to *ca.* 600 cm^{-1} and are dominant in the IR spectra, obscuring the signals of the bending modes of the methyl groups C–H.^{30a,32}

In the ¹H NMR spectra of salts of the (*E*)-N₄Me₄H⁺ cation (**2** and **3**) in DMSO-*d*₆, two resonances are observed at *ca.* 3.05 ppm for the protons of the methyl groups and at 13.19 (**2**) and 11.51 ppm (**3**) for the proton of the nitrogen atom. Note the low field shift of the resonance of the N–H proton in compound **2** in comparison to **3**, in agreement with the higher acidity of hydrochloric acid in comparison to picric acid. In the ¹³C NMR spectra, both **2** and **3** show only one signal for the carbon atoms of the methyl groups at *ca.* 34 ppm. By comparison, (*E*)-N₄Me₄ (**1**) has resonances at 2.72 (¹H NMR) and *ca.* 39.9 (¹³C NMR) ppm. The extra methyl group in the (*E*)-N₄Me₅⁺ cation of compound **4** in comparison to the (*E*)-N₄Me₄H⁺ cation of salts **2** and **3**, results in loss of symmetry and the carbon and hydrogen atoms of the –NMe₂ and –NMe₃ fragments show different resonances. In the ¹H NMR spectrum two resonances are observed at 3.12 (–NMe₃) and 3.49 (–NMe₂) ppm. In analogy, the ¹³C NMR spectrum of **4** also shows two resonances for the carbon atoms, which can be found at 38.1 (–NMe₂) and 42.4 (–NMe₃) ppm. Lastly, all compounds **2**, **3** and **4** were too insoluble or unstable in any solvent tried to record a ¹⁵N NMR spectrum (natural abundance).

Geometry and NBO analysis of (*E*)-N₄Me₄ (**1**) and the (*E*)-N₄Me₄H⁺ and (*E*)-N₄Me₅⁺ cations

The optimized geometry of (*E*)-N₄Me₄ (**1**) and the (*E*)-N₄Me₄H⁺ and (*E*)-N₄Me₅⁺ cations was obtained as described above (see Computational Details section) and used for the natural bond orbital (NBO) calculations. Table 1 contains a summary of the bond distances and angles calculated for the optimized (gas phase) structures of (*E*)-N₄Me₄ (**1**) and the (*E*)-N₄Me₄H⁺ and (*E*)-N₄Me₅⁺ cations (see Fig. 2–4 for the labelling scheme of all three species). The optimized geometry of (*E*)-N₄Me₄ (**1**) shows N–N distances for the terminal nitrogen atoms of N1–N2 = N3–N4 = 1.377 Å between N–N single (1.454 Å) and N=N double bonds (1.245 Å).³³ The azo bridge distance (N2–N3 = 1.257 Å) is slightly longer than the average N=N double bond and comparable to the analogous X-ray distances found in salts of the 5,5'-azotetrazolate anion.³⁴ As expected, the C–N distances (1.457 Å) are typical for C–N single bonds (1.47 Å).¹⁹ Protonation/methylation of **1** to form the (*E*)-N₄Me₄H⁺ and (*E*)-N₄Me₅⁺ cations, respectively, results, in a significant weakening (lengthening) of the bond distances

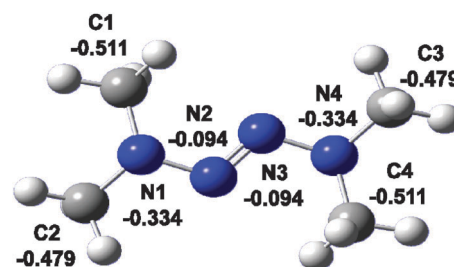


Fig. 2 Optimized geometry and charge distribution in (*E*)-N₄Me₄ (**1**) as found with NBO analysis (B3LYP/6-31+G(d,p)).

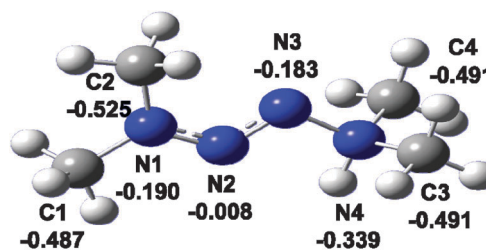


Fig. 3 Optimized geometry and charge distribution for the (*E*)-N₄Me₄H⁺ cation as found with NBO analysis (B3LYP/6-31+G(d,p)).

Table 1 Selected optimized geometry parameters for (*E*)-N₄Me₄ (**1**) and the (*E*)-N₄Me₄H⁺ and (*E*)-N₄Me₅⁺ cations in the gas phase (B3LYP/6-31+G(d,p))^a

	(<i>E</i>)-N ₄ Me ₄ (1)	(<i>E</i>)-N ₄ Me ₄ H ⁺	(<i>E</i>)-N ₄ Me ₅ ⁺		(<i>E</i>)-N ₄ Me ₄ (1)	(<i>E</i>)-N ₄ Me ₄ H ⁺	(<i>E</i>)-N ₄ Me ₅ ⁺
<i>R</i> (N1–N2)	1.377	1.294	1.296	<i>R</i> (N4–C3)	1.457	1.500	1.505
<i>R</i> (N1–C2)	1.457	1.465	1.465	<i>R</i> (N4–C4)	1.457	1.500	1.505
<i>R</i> (N1–C1)	1.457	1.465	1.465	<i>R</i> (N2–N3)	1.257	1.277	1.272
<i>R</i> (N4–N3)	1.377	1.477	1.507	<i>R</i> (N4–C5)			1.502
<i>A</i> (N2–N1–C2)	118.4	109.2	121.7	<i>A</i> (N1–N2–N3)	114.1	106.0	115.9
<i>A</i> (N2–N1–C1)	110.9	109.2	117.4	<i>A</i> (N4–N3–N2)	114.1	116.3	107.8
<i>A</i> (C2–N1–C1)	116.0	112.9	121.0	<i>A</i> (N3–N4–C5)			103.4
<i>A</i> (N3–N4–C3)	118.4	121.6	110.9	<i>A</i> (C3–N4–C5)			110.2
<i>A</i> (N3–N4–C4)	110.9	117.2	110.9	<i>A</i> (C4–N4–C5)			110.2
<i>A</i> (C3–N4–C4)	116.0	121.1	110.9				

^a *R* = bond distance (in Å), *A* = bond angle (in °).

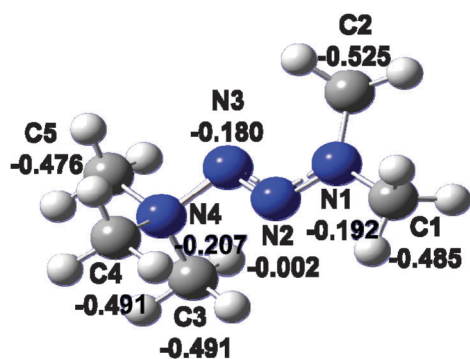


Fig. 4 Optimized geometry and charge distribution for the (*E*)- $N_4Me_5^+$ cation as found with NBO analysis (B3LYP/6-31+G(d,p)).

around the protonated/methylated nitrogen atom (N4), which is more accentuated in the case of the (*E*)- $N_4Me_5^+$ cation (N3–N4 = 1.507 Å and C3–N4 = C4–N4 = 1.505 Å) than for the (*E*)- $N_4Me_4H^+$ cation (N3–N4 = 1.477 Å and C3–N4 = C4–N4 = 1.500 Å). In contrast, the N–N bond distance of the non-protonated/non-methylated terminal nitrogen atom (N1) is significantly shorter for the (*E*)- $N_4Me_4H^+$ and the (*E*)- $N_4Me_5^+$ cations (N1–N2 = 1.294 Å and 1.296 Å, respectively) than for **1**. Lastly, the azo N2–N3 distances and the remainder of the C–N distances are comparable in all three species.

Tables 2 and 3 contain a summary of the electronic and zero point energies as well as the dipole moment of the (*E*)- $N_4Me_4H^+$ and (*E*)- $N_4Me_5^+$ cations. According to our B3LYP calculations,

both the (*E*)- $N_4Me_4H^+$ and (*E*)- $N_4Me_5^+$ cations with the proton/methyl group at N1 or N4 positions, have approximately the same electronic and zero point energies. However, the conformations with the proton/methyl group at N2 or N3 positions, have different energies between them and are predicted to be less stable by 51.4 and 55.6 kcal mol⁻¹ ((*E*)- $N_4Me_4H^+$ cation protonated at N3 and N2, respectively) and by 71.6 and 80.2 kcal mol⁻¹ ((*E*)- $N_4Me_5^+$ cation methylated at N3 and N2, respectively). Note that the electronic energy calculated by Porath *et al.*¹⁶ for **1** (–378.59825990 a.u.) points at the protonation/methylation of **1** playing a stabilizing role.

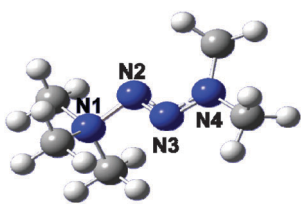
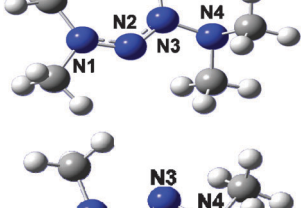
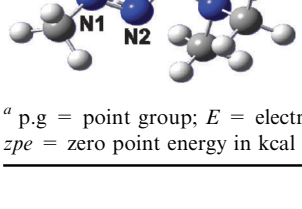
Fig. 2–4 show the calculated NBO charges for (*E*)- N_4Me_4 (**1**) and the (*E*)- $N_4Me_4H^+$ and (*E*)- $N_4Me_5^+$ cations. For (*E*)- N_4Me_4 (**1**), the azo bridge nitrogen atoms (N2 and N3) bear small negative charges (–0.094e) in contrast to the terminal nitrogen atoms (N1 and N4) that hold a more negative charge of –0.334e. The more negative charge of the terminal nitrogen atoms supports the conclusion that protonation/methylation will be easier on these atoms, in keeping with the results of the calculated energies of the (*E*)- $N_4Me_4H^+$ and (*E*)- $N_4Me_5^+$ cations (see discussion above). This finding is also supported by previous studies that report high proton affinities for tetrasubstituted 2-tetrazenes and an appreciable electron density concentration at the terminal nitrogen atoms.³⁵ Unfortunately, we were not able to grow high quality single crystals of compounds **2–4**, however, low quality single crystals of the iodide salt **4** showed a “ N_4Me_2 ” fragment and an iodide anion. We assume that the high electron density of iodine

Table 2 Computational results for the (*E*)- $N_4Me_4H^+$ cation using DFT calculations (B3LYP/6-31+G(d,p))^a

Species	Formula	p.g	– <i>E</i>	Δ	<i>zpe</i>	<i>NI</i>	μ
	[Me ₂ N–N=N–NHMe ₂] ⁺	C ₁	378.98013950	0	118.92	0	2.5088
	[Me ₂ N–N=N–NH–NMe ₂] ⁺	C ₁	378.95897678	55.6	117.82	0	3.9485
	[Me ₂ N–NH=N–NMe ₂] ⁺	C ₁	378.96054150	51.4	118.13	0	2.6372
	[Me ₂ NH–N=N–NMe ₂] ⁺	C ₁	378.98013950	0	118.92	0	2.5086

^a p.g = point group; *E* = electronic energy in atomic units; Δ = destabilization energy relative to the most favourable isomer in kcal mol⁻¹; *zpe* = zero point energy in kcal mol⁻¹; *NI* = number of imaginary frequencies; μ = dipole moment in Debye.

Table 3 Computational results for the (*E*)-N₄Me₅⁺ cation using DFT calculations (RB3LYP/6-31+G(d,p))^a

Species	Formula	p.g.	- <i>E</i>	<i>A</i>	<i>zpe</i>	<i>NI</i>	<i>μ</i>
	[Me ₂ N-N=N-NMe ₃] ⁺	C ₁	418.29313426	0	136.23	0	1.7643
	[Me ₂ N-N=NMe-NMe ₂] ⁺	C ₁	418.26256972	80.2	135.72	0	3.5831
	[Me ₂ N-NMe=N-NMe ₂] ⁺	C ₁	418.26587491	71.6	135.77	0	2.9582
	[Me ₃ N-N=N-NMe ₂] ⁺	C ₁	418.29313424	5.2 × 10 ⁻⁵	136.23	0	1.7646

^a p.g. = point group; *E* = electronic energy in atomic units; *A* = destabilization energy relative to the most favourable isomer in kcal mol⁻¹; *zpe* = zero point energy in kcal mol⁻¹; *NI* = number of imaginary frequencies; *μ* = dipole moment in Debye.

did not allow to locate the three missing methyl groups but they are probably placed on N4, confirming the results of our calculations. On the other hand, protonation/methylation results in loss of symmetry in comparison to **1** and while one of the azo nitrogen atoms (N2) carries an almost neutral charge in both the (*E*)-N₄Me₄H⁺ and (*E*)-N₄Me₅⁺ cations, the other azo nitrogen atom (N3) carries a significant negative charge in both species (*ca.* -0.180e). In a similar way, the protonated/methylated nitrogen atom (N4) bears a more significant negative charge than the other terminal nitrogen atom (N1). Note that the charge of the protonated nitrogen atom (N4) in the (*E*)-N₄Me₄H⁺ cation (-0.339e) does not differ significantly from that of **1** (-0.334e), which is in contrast with classical chemistry, which describes a tetra-coordinated nitrogen atom as being positively charged. This interpretation to explain the quadricovalency of the nitrogen atoms is misleading in conjugate acids because the positive charge is uniformly distributed in this type of compounds.³⁹ Lastly, similar trends are observed for the Mulliken charges (Fig. 1–3 of the ESI[†]).

Decomposition of **3** in hot water

As mentioned above, when dissolving **3** in water at room temperature, no appreciable decomposition was observed, however, when the compound was dissolved in hot water and the solvent was left to evaporate, single crystals of dimethylammonium picrate were obtained (see Fig. 5). This decomposition is in agreement with previous studies, which

suggest tetraalkyl-2-tetrazenes might decompose to form two entities of the dialkylammonium radical (R₂N^{•+}) and molecular nitrogen^{23,36} and suggest the following mechanism for the decomposition of **3** (see Scheme 2).¹⁶

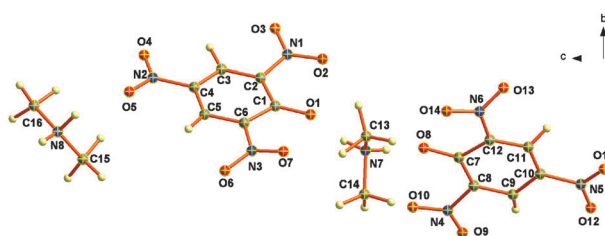
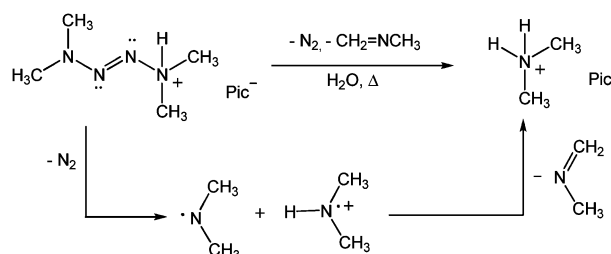


Fig. 5 Asymmetric unit of dimethylammonium picrate with the labeling scheme (diamond ellipsoids at 50% probability).



Scheme 2 Proposed mechanism for the decomposition reaction of picrate salt **3** in hot water. Pic⁻ = picrate anion.

The crystal structure of dimethylammonium picrate has already been reported in the literature,³⁷ therefore, only attention to the hydrogen-bonding networks is paid here. X-Ray quality crystals of the compound were obtained as described above. Table SI 5 (ESI†) shows a summary of the hydrogen-bonding graph-sets found in the structure of the compound. The formation of dimeric networks is dominant. These take the descriptors **D1,1(2)**, **D1,2(3)** and **D2,2(X)** ($X = 5, 7, 9$). Additionally, ring graph-sets of the type **R2,1(6)** are also formed (Fig. 6), which are reminiscent to those found in the crystal structure of azolium salts of the same anion.^{29b}

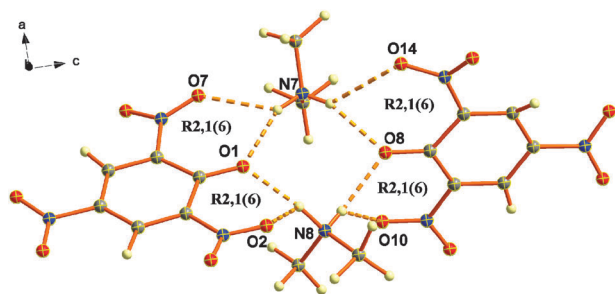


Fig. 6 Ring hydrogen-bonding networks in the crystal structure of dimethylammonium picrate.

Conclusions

From this combined experimental and theoretical study, the following conclusions can be drawn:

We synthesized two salts of the $(E)\text{-N}_4\text{Me}_4\text{H}^+$ cation with chloride (**2**) and picrate (**3**) anions and the iodide salt of the $(E)\text{-N}_4\text{Me}_5^+$ cation (**4**) and characterized the compounds extensively by analytical (elemental analysis and mass spectrometry) and spectroscopic methods (IR, Raman, NMR and UV). The low thermal stability of compounds **2–4** as the pure solids and in several solvents is in agreement with the low decomposition temperatures obtained from the DSC measurements. NBO analysis on $(E)\text{-N}_4\text{Me}_4$ (**1**) anticipate a high concentration of electron density on the terminal nitrogen atoms, which suggest these atoms as the most likely to undergo protonation/methylation to form the $(E)\text{-N}_4\text{Me}_4\text{H}^+$ and the $(E)\text{-N}_4\text{Me}_5^+$ cations. These results are in agreement with the DFT energy calculations for the $(E)\text{-N}_4\text{Me}_4\text{H}^+$ and the $(E)\text{-N}_4\text{Me}_5^+$ cations, that predict the conformations with the proton/methyl group on the terminal nitrogen atom to be the most stable, and fit the experimental observations. Additionally, the long N3–N4 distances calculated for the optimized geometries of the $(E)\text{-N}_4\text{Me}_4\text{H}^+$ and the $(E)\text{-N}_4\text{Me}_5^+$ cations in comparison to the analogous distances in $(E)\text{-N}_4\text{Me}_4$ (**1**), suggest this bond to be the initiating point for the decomposition of 2-tetrazenium salts to form molecular nitrogen and ammonium salts, as supported by the formation of dimethylammonium picrate upon decomposition of **3** in hot water. These results suggest the formation of dialkylammonium radicals ($\text{R}_2\text{N}^+\bullet$) during the decomposition pathway of **3**. Lastly, the low thermal stability of compounds **2–4** limits their application in the field of energetic materials, however, salts **2** and **4** should be regarded as valuable intermediates for the synthesis of salts of the energetically interesting $(E)\text{-N}_4\text{Me}_4\text{H}^+$ and $(E)\text{-N}_4\text{Me}_5^+$ cations. In particular, combination of the

$(E)\text{-N}_4\text{Me}_4\text{H}^+$ and $(E)\text{-N}_4\text{Me}_5^+$ cations with larger and nitrogen-rich anions, which might have the possibility of stabilizing the materials *via* electrostatic dipole–dipole interactions, are expected to have improved thermal stabilities. We are currently studying the effect of several anions in the thermal stability of the resulting 2-tetrazenium salts. The results of this work will be presented in a future report.

Experimental section

Safety note

2-Tetrazenes and their derivatives are potentially explosive compounds. Preliminary testing showed decreased sensitivities towards impact and friction, however, we recommend care to be taken at all times, particularly, when working on a large scale. We further recommend the synthesis of the compounds reported here to be carried out only by experienced personnel using non-conductive equipment (*e.g.*, plastic spatulas and plastic wear) and wearing safety gear such as Kevlar gloves and jacket, conductive shoes and face shield.

X-Ray measurements

The crystallographic data of dimethylammonium picrate were collected using an Oxford Diffraction Xcalibur 3 diffractometer, which was equipped with a CCD detector using the CrysAlis CCD software.³⁸ For the data reduction, the CrysAlis RED software³⁹ was used and the structure was solved using the WinGX software.^{40,41} The non-hydrogen atoms were refined anisotropically and we applied a multi-scan absorption correction.⁴² Ref. 43 contains a summary of the results of the crystal structure and refinement. Lastly, the geometry of the hydrogen bonds and the results of the graph-set analysis^{44,45} have been collected in Tables 4 and 5 of the ESI†.

Computational details

The (gas phase) geometry of $(E)\text{-N}_4\text{Me}_4$ (**1**) and the $(E)\text{-N}_4\text{Me}_4\text{H}^+$ and $(E)\text{-N}_4\text{Me}_5^+$ cations (*i.e.*, $(E)\text{-N}_4\text{Me}_4$ (**1**) protonated/methylated at the N4 position) was optimized using DFT calculations with the B3LYP method^{46,47} at the 6-311+G(d,p) level of theory. For all three geometries no imaginary frequencies were found and the potential energy surface showed a true minimum. The optimized geometries of $(E)\text{-N}_4\text{Me}_4$ (**1**) and the $(E)\text{-N}_4\text{Me}_4\text{H}^+$ and $(E)\text{-N}_4\text{Me}_5^+$ cations were subsequently used to calculate the harmonic vibrational frequencies with infrared (IR) intensities and Raman activities using the computer program Gaussian 03W.⁴⁸ A scaling factor of 0.9613, as suggested by Scott and Radom for calculations using B3LYP/6-311+G(d,p),⁴⁹ was used for the computed frequencies. In addition, we performed a natural bond (NBO) analysis on the optimized structures of $(E)\text{-N}_4\text{Me}_4$ (**1**) and the $(E)\text{-N}_4\text{Me}_4\text{H}^+$ and $(E)\text{-N}_4\text{Me}_5^+$ cations using the option implemented in Gaussian 03W.

General method

All chemical reagents and solvents of analytical grade were obtained from Sigma-Aldrich Inc. or Acros Organics and used as supplied. ^1H and ^{13}C NMR spectra were recorded on a JEOL Eclipse 400 instrument. The chemical shifts are given

relative to tetramethylsilane as an external standard. Infrared (IR) spectra were recorded at room temperature on a Perkin-Elmer Spectrum instrument equipped with a Universal ATR sampling accessory. Raman spectra were recorded on a Perkin-Elmer Spectrum 2000R NIR FT-Raman instrument equipped with a Nd:YAG laser (1064 nm). IR intensities are given in parentheses as vw = very weak, w = weak, m = medium, s = strong and vs = very strong. Raman activities are reported in percentages relative to the most intense peak and are given in parentheses. Elemental analyses were performed with a Netsch Simultaneous Thermal Analyzer STA 429. The thermal behaviour was analysed by differential scanning calorimetry (SETARAM DSC131 instrument, calibrated with standard pure indium and zinc) at a heating rate of $\beta = 5\text{ }^{\circ}\text{C min}^{-1}$ in closed aluminium containers and with a nitrogen flow of 20 mL min^{-1} . The reference sample was a closed aluminium container.

Syntheses

(E)-1,1,4,4-Tetramethyl-2-tetrazene (1). **1** was synthesized according to a literature procedure.²³ $\text{C}_4\text{H}_{12}\text{N}_4$ (MW = 116.16 g mol^{-1} , calc./found): C 41.35/41.28, H 10.42/10.40, N 48.23/48.06%; $^1\text{H NMR}$ (CDCl_3 , 400.18 MHz, TMS) δ/ppm : 2.72 (12 H, s, $-\text{CH}_3$); Raman $\tilde{\nu}/\text{cm}^{-1}$ (rel. int.): 202(11), 328(10), 372(10), 458(6), 584(5), 897(21), 1036(1), 1090(1), 1142(25), 1240(1), 1290(1), 1395(9), 1415(27), 1443(15), 1473(100), 2777(31), 2822(31), 2853(33), 2883(29), 2962(72), 2999(22), 3088(13); IR $\tilde{\nu}/\text{cm}^{-1}$ (golden gate, rel. int.): 2999(vw) 2961(w) 2857(w) 2822(w) 2788(vw) 1633(vw) 1593(vw) 1469(m) 1441(w) 1399(vw) 1277(m) 1244(w) 1141(m) 1091(vw) 1037(w) 997(vs) 891(w) 822(m) 591(s).

(E)-1,1,4,4-Tetramethyl-2-tetrazenium chloride (2). Compound **1** (0.238 g, 2.0 mmol) was dissolved in diethyl ether (4 mL) under exclusion of air to give a slightly yellow solution. A 2 N ethereal hydrochloric acid solution (1.0 mL, 2.0 mmol) was added dropwise resulting in a slightly exothermic reaction and the immediate precipitation of a colorless solid. After the addition was finished, the reaction mixture was stirred at room temperature for 10 min and the insoluble material was filtered under vacuum, washed with diethyl ether ($2 \times 2\text{ mL}$) and dried under vacuum. The title compound was obtained as a colorless powder (0.295 g, 97%) and no further purification was necessary. $\text{C}_4\text{H}_{13}\text{N}_4\text{Cl}$ (MW = 152.63 g mol^{-1} , calc./found): C 31.48/31.09, H 8.58/8.37, N 36.71/36.44; DSC ($5\text{ }^{\circ}\text{C min}^{-1}$): one exothermic peak (sharp, peak onset: $56.61\text{ }^{\circ}\text{C}$, peak maximum: $59.67\text{ }^{\circ}\text{C}$, $\Delta H = -296.97\text{ J g}^{-1}$); m/z (FAB⁺, Xenon, 6 keV, *m*-NBA matrix): 117.0 ($\text{N}_4\text{Me}_4\text{H}^+$); $^1\text{H NMR}$ (DMSO- $[\text{D}_6]$, 400.18 MHz, TMS) δ/ppm : 3.05 (s, 12 H, $-\text{CH}_3$), 13.19 (s(br), 1 H, $-\text{NH}$); $^{13}\text{C}\{^1\text{H}\}$ NMR (DMSO- d_6 , 100.63 MHz, $25\text{ }^{\circ}\text{C}$, TMS) δ/ppm : 33.6 (4 C, CH_3); Raman $\tilde{\nu}/\text{cm}^{-1}$ (rel. int.): 78(25), 96(21), 178(11), 245(5), 327(26), 364(7), 426(4), 502(12), 541(5), 620(2), 711(1), 820(3), 898(33), 952(3), 1005(6), 1064(1), 1106(24), 1375(35), 1385(100), 1452(18), 1702(3), 1762(2), 1786(1), 2292(3), 2790(2), 2840(3), 2963(25), 3006(21), 3021(14); IR $\tilde{\nu}/\text{cm}^{-1}$ (golden gate, rel. int.): 3016(w) 3001(w) 2954(w) 2917(w) 2780(vw) 2526(w) 2492(w) 2356(m) 2274(m) 2121(m) 1487(m) 1456(m) 1446(m) 1433(w) 1414(w) 1397(m) 1380(m) 1357(s) 1297(w) 1229(w) 1188(w) 1177(m) 1129(vw) 1102(w)

1062(w) 1045(w) 1001(m) 947(m) 895(w) 814(w) 677(w) 617(vs) 575(vw) 566(vw); UV (water, $7.86 \times 10^{-5}\text{ M}$, nm): 239 ($\epsilon = 7904\text{ L mol}^{-1}\text{ cm}^{-1}$).

(E)-1,1,4,4-Tetramethyl-2-tetrazenium picrate (3). Compound **1** (780 μL , 0.701 g, 6.04 mmol) was added dropwise to a suspension of picric acid (1.374 g, 6.00 mmol) in ether (50 mL) causing the immediate precipitation of a bright yellow powder and the formation of a bright yellow solution. The insoluble compound was filtered after stirring for *ca.* 1 h, washed with little ether and dried under high vacuum. No further purification was necessary (1.960 g, 95%). ρ (picnometer, $17.4\text{ }^{\circ}\text{C}$): 1.440 g cm^{-3} ; $\text{C}_{10}\text{H}_{15}\text{N}_7\text{O}_7$ (MW = 345.27 g mol^{-1} , calc./found): C 34.78/34.79, H 4.38/4.31, N 28.40/28.23; DSC ($5\text{ }^{\circ}\text{C min}^{-1}$): two exothermic peaks (peak 1: sharp, onset: $72.50\text{ }^{\circ}\text{C}$, peak maximum: $76.64\text{ }^{\circ}\text{C}$, $\Delta H = -442.66\text{ J g}^{-1}$; peak 2: broad, onset: $231.76\text{ }^{\circ}\text{C}$, peak maximum: $253.76\text{ }^{\circ}\text{C}$, $\Delta H = -560.36\text{ J g}^{-1}$); m/z ($-c$ ESI): 228.1 (76, A^-), 478.9 (17, $[\text{A}_2\text{Na}]^-$), 708.0 (19), 724.0 (25), 729.8 (78, $[\text{A}_3\text{Na}_2]^-$), 974.7 (100), 1225.5 (15), 1476.1 (4); m/z ($+c$ ESI): 74.0 (15, $[\text{Cat} - \text{N}(\text{CH}_3)_2]^+$), 102.1 (100, $[\text{Cat} - \text{CH}_3]^+$), 126.9 (18), 201.9 (12), 273.9 (14); $^1\text{H NMR}$ (DMSO- d_6 , 400.18 MHz, $25\text{ }^{\circ}\text{C}$, TMS) δ/ppm : 11.51 (s(br), 1 H, $-\text{NH}$), 8.58 (2 H, s, H-aromat.), 3.04 (12 H, s, CH_3); $^{13}\text{C}\{^1\text{H}\}$ NMR (DMSO- d_6 , 100.63 MHz, $25\text{ }^{\circ}\text{C}$, TMS) δ/ppm : 160.9 (1 C, C1), 141.7 (2 C, C2), 125.3 (2 C, C3), 124.5 (1 C, C4), 34.4 (4 C, CH_3); Raman $\tilde{\nu}/\text{cm}^{-1}$ (rel. int.): 78(11), 175(6), 193(4), 327(5), 536(1), 823(4), 917(2), 944(2), 1085(2), 1168(7), 1240(1), 1295(33), 1315(100), 1360(2), 1405(1), 1514(2), 1549(7), 1611(2), 2956(2), 2968(1); IR $\tilde{\nu}/\text{cm}^{-1}$ (golden gate, rel. int.): 3082(w) 3023(w) 2960(w) 2441(w) 1633(w) 1606(m) 1562(m) 1538(m) 1494(m) 1434(m) 1405(w) 1384(m) 1384(m) 1361(m) 1314(s) 1271(vs) 1238(m) 1182(m) 1162(m) 1112(m) 1079(m) 1053(m) 1004(w) 942(w) 913(m) 837(w) 818(w) 791(m) 770(w) 743(m) 721(m) 709(vs) 670(m) 620(m); UV (water, $7.33 \times 10^{-5}\text{ M}$, nm): 235 ($\epsilon = 20520\text{ L mol}^{-1}\text{ cm}^{-1}$).

(E)-1,1,1,4,4-Pentamethyl-2-tetrazenium iodide (4)⁵⁰. Compound **1** (1.290 mL, 1.16 g, 9.99 mmol) was loaded in a 10 mL round-bottom flask and cooled to $0\text{ }^{\circ}\text{C}$ by means of a water/ice bath. At this point, previously cooled methyl iodide (0.615 mL, 1.42 g, 10.00 mmol) was added dropwise with strong stirring (*careful*, very exothermic reaction!). Immediate cloudiness was observed and a white precipitate formed after a few minutes. The reaction mixture was stirred for *ca.* 15 min at $0\text{ }^{\circ}\text{C}$ and the white precipitate was filtered at this temperature, washed with ether and vacuum-dried (1.158 g, 45%). Low quality single crystals were grown by dissolving **4** in dry ethanol and storing in an ether chamber in the fridge over two weeks. $\text{C}_5\text{H}_{15}\text{N}_4\text{I}$ (MW = 258.10 g mol^{-1} , calc./found): C 23.27/22.94, H 5.86/5.53, N 21.71/21.09; DSC ($5\text{ }^{\circ}\text{C min}^{-1}$): one exothermic peak (sharp, peak onset: $52.15\text{ }^{\circ}\text{C}$, EX. dec.); m/z (ESI⁺): 46.0 (5, $[\text{Me}_2\text{NH}_2]^+$), 60.1 (26, $[\text{Me}_3\text{NH}]^+$), 74.1 (2, $[\text{Me}_2\text{N} - \text{N} = \text{NH}_2]^+$), 87.1 (3, $[\text{Cat}^+ - \text{Me}_2\text{N}]^+$), 116.1 (10, $[\text{Cat}^+ - \text{Me}]^+$), 128.1 (14, Cat^+), 219.0 (77, $[2\text{ Cat}^+ - \text{HN}_3]^+$), 233.1 (100, $[2\text{ Cat}^+ - \text{HN}_2]^+$), 247.1 (75, $[2\text{ Cat}^+ - \text{HN}]^+$), 261.2 (52, $[2\text{ Cat}^+ - \text{H}^+]^+$); m/z (ESI⁻): 126.9 (37, I^-), 254.8 (12, $[2\text{ I}^- + \text{H}^+]^-$), 276.8 (19, $[2\text{ I}^- + \text{Na}^+]^-$), 285.9 (20), 299.9 (100), 380.7 (31); $^1\text{H NMR}$ (DMSO- $[\text{D}_6]$, 400.18 MHz,

TMS) δ /ppm: 3.12 (s, 9 H, $-\text{CH}_3$), 3.49 (s, 6 H, $-\text{CH}_3$); $^{13}\text{C}\{^1\text{H}\}$ NMR (DMSO- d_6 , 100.63 MHz, 25 °C, TMS) δ /ppm: 42.4 (3 C, CH_3), 38.1 (2 C, CH_3); Raman $\tilde{\nu}/\text{cm}^{-1}$ (rel. int.): 291(13), 343(8), 384(4), 420(4), 495(3), 562(7), 777(9), 825(9), 916(3), 949(1), 966(4), 1106(5), 1145(3), 1251(5), 1304(3), 1364(6), 1396(21), 1427(11), 1444(9), 1475(37), 2730(2), 2762(1), 2791(5), 2840(11), 2945(92), 3008(100), 3018(86); IR $\tilde{\nu}/\text{cm}^{-1}$ (golden gate, rel. int.): 3071(w) 3010(w) 2945(w) 2356(w) 2182(w) 2168(w) 2042(w) 1963(w) 1946(w) 1704(w) 1629(w) 1598(w) 1555(w) 1482(m) 1461(m) 1439(w) 1407(m) 1385(s) 1361(m) 1299(w) 1261(m) 1229(m) 1139(w) 1113(w) 1101(m) 1049(w) 968(m) 948(m) 908(m) 820(w) 775(m) 746(w) 707(w) 638(w) 589(s) 558(w) 497(w) 473(w) 463(w).

Acknowledgements

Financial support by the Centre Nationale de la Recherche Scientifique (CNRS), the Centre Nationale d'Études Spatiales (CNES), the Société Nationale des Poudres et des Explosifs (SNPE) and the University Claude Bernard of Lyon are gratefully acknowledged.

Notes and references

- 1 T. M. Klapötke, P. Mayer, C. Miró Sabaté, J. M. Welch and N. Wiegand, *Inorg. Chem.*, 2008, **47**(13), 6014–6027; T. M. Klapötke, C. Miró Sabaté and J. Stierstorfer, *Z. Anorg. Allg. Chem.*, 2008, **11**, 1867–1874; M. von Denffer, T. M. Klapötke and C. Miró Sabaté, *Z. Anorg. Allg. Chem.*, 2008, **634**, 2575–2582; T. M. Klapötke, C. Miró Sabaté and M. Rasp, *Dalton Trans.*, 2009, 1825–1834; T. M. Klapötke and C. Miró Sabaté, *Dalton Trans.*, 2009, 1835–1841; M. Ebespächer, T. M. Klapötke and C. Miró Sabaté, *Helv. Chim. Acta*, 2009, **92**, 977–996; T. M. Klapötke, C. Miró Sabaté and J. M. Welch, *Eur. J. Inorg. Chem.*, 2009, 769–776; M. Ebespächer, T. M. Klapötke and C. Miró Sabaté, *New J. Chem.*, 2009, **33**, 517–527; H. Delalu, K. Karaghiosoff, T. M. Klapötke and C. Miró Sabaté, *Cent. Eur. J. Energ. Mater.*, 2010, **7**(3), 115–129.
- 2 T. M. Klapötke, P. Mayer, A. Schulz and J. J. Weigand, *Propellants, Explos., Pyrotech.*, 2004, **29**, 325–332; D. L. Strout, *J. Phys. Chem. A*, 2004, **108**, 10911–10916; M. H. V. Huynh, M. A. Hiskey, E. L. Hartline, D. P. Montoya and R. Gilardi, *Angew. Chem.*, 2004, **116**, 5032–5036 (*Angew. Chem., Int. Ed.*, 2004, **43**, 4924–4928); R. Haiges, S. Schneider, T. Schroer and K. O. Christe, *Angew. Chem.*, 2004, **116**, 5027–5032 (*Angew. Chem., Int. Ed.*, 2004, **43**, 4919–4924).
- 3 R. P. Singh, R. D. Verma, D. T. Meshri and J. M. Shreeve, *Angew. Chem.*, 2006, **118**, 3664–3682 (*Angew. Chem., Int. Ed.*, 2006, **45**, 3584–3601); T. M. Klapötke, *Structure and Bonding*, Springer, Berlin/Heidelberg, Germany, 2007; G. Drake, *US Pat.*, 6 509 473, 2003; V. A. Dulles and G. Drake, *AFOSSR Ionic Liquids Workshop*, Aberdeen, MD, 2003.
- 4 T. Abe, Y.-H. Joo, G.-H. Tao and J. M. Shreeve, *Chem.-Eur. J.*, 2009, **15**, 4102–4110; Y.-H. Joo and J. M. Shreeve, *Eur. J. Org. Chem.*, 2009, 3573–3578; G.-H. Tao, Y.-H. Joo, B. Twamley and J. M. Shreeve, *J. Mater. Chem.*, 2009, **19**, 5850–5854; Y. Guo, G.-H. Tao, Z. Zeng, H. Gao and J. M. Shreeve, *Chem.-Eur. J.*, 2010, **16**, 3753–3762; G.-H. Tao, Y. Guo, D. A. Parrish and J. M. Shreeve, *J. Mater. Chem.*, 2010, **20**, 2999–3005; Y.-H. Joo and J. M. Shreeve, *Angew. Chem., Int. Ed.*, 2010, **49**, 7320–7323; Y.-H. Joo and J. M. Shreeve, *J. Am. Chem. Soc.*, 2010, **132**, 15081–15090.
- 5 H. Gao, C. Ye, R. W. Winter, G. L. Gard, M. E. Sitzmann and J. M. Shreeve, *Eur. J. Inorg. Chem.*, 2006, 3221–3226; Y. Gao, C. F. Ye, B. Twamley and J. M. Shreeve, *Chem.-Eur. J.*, 2006, **12**, 9010–9018; G. Gao, R. Wang, B. Twamley, M. A. Hiskey and J. M. Shreeve, *Chem. Commun.*, 2006, 4007–4009; Y. Huang, H. Gao, B. Twamley and J. M. Shreeve, *Eur. J. Inorg. Chem.*, 2007, 2025–2030; R. W. Wang, H. Gao, C. Ye, B. Twamley and J. M. Shreeve, *Inorg. Chem.*, 2007, **46**, 932–938.
- 6 G. Kaplan, G. Drake, K. Tollison, L. Hall and T. Hawkins, *J. Heterocycl. Chem.*, 2005, **42**, 19–27; H. Oestmark, *Proceedings of the 9th Seminar on New Trends in the Research of Energetic Materials*, Institute of Energetic Materials, University of Pardubice, Czech Republic, April 19–21, 2006.
- 7 J. Uddin, V. Barone and G. E. Scuseria, *Mol. Phys.*, 2006, **104**, 745–749; H. Oestmark, S. Walin and P. Goede, *Cent. Eur. J. Energ. Mater.*, 2007, **4**, 83–108.
- 8 H. Feuer and A. T. Nielsen, *Nitro Compounds*, Wiley-VCH, Weinheim, Germany, 1990.
- 9 A. T. Nielsen, *Nitrocarbons*, Wiley-VCH, Weinheim, Germany, 1995.
- 10 D. E. Chavez, M. A. Hiskey and R. D. Gilardi, *Angew. Chem., Int. Ed.*, 2000, **39**, 1861–1863.
- 11 A. Hammerl, T. M. Klapötke, H. Nöth, M. Warchhold, G. Holl and M. Kaiser, *Inorg. Chem.*, 2001, **40**, 3570–3575.
- 12 International Conference on Green Propellant for Space Propulsion, Noordwijk, The Netherlands, June 20–22, 2001; <http://esamultimedia.esa.int/conferences/01a05/index.html>.
- 13 A. K. Sikder and N. Sikder, *J. Hazard. Mater.*, 2004, **A112**, 1–15.
- 14 H. Gao, Y. Huang, C. Ye, B. Twamley and J. M. Shreeve, *Chem.-Eur. J.*, 2008, **14**, 5596–5603.
- 15 (a) T. M. Klapötke, P. Mayer, A. Schulz and J. J. Weigand, *Propellants, Explos., Pyrotech.*, 2004, **29**, 325; (b) J. Heppekaussen, T. M. Klapötke and S. M. Sproll, *J. Org. Chem.*, 2009, **74**, 2460–2466; (c) B. Porath, P. Rademacher, R. Böse and D. Bläser, *Z. Naturforsch., B: Chem. Sci.*, 2002, **57**, 365–376; (d) B. Rose, D. Schollmeyer and H. Meier, *Liebigs Ann./Recl.*, 1997, 409–412.
- 16 B. Porath, R. Munzenberg, P. Heymans, P. Rademacher, R. Böse, D. Bläser and R. Latz, *Eur. J. Org. Chem.*, 1998, 1431–1440 and references therein.
- 17 W. E. Bull, H. A. Seaton and L. F. Audrieth, *J. Am. Chem. Soc.*, 1958, **80**, 2516–2518.
- 18 N. Wiberg, H. Bayer and H. Bachhuber, *Angew. Chem.*, 1975, **87**(6), 202–203; N. Wiberg, H. W. Haering and S. K. Vasisht, *Z. Naturforsch. B: Anorg. Chem. Org. Chem.*, 1979, **34**(2), 356–357.
- 19 A. F. Holleman, E. Wiberg and N. Wiberg, *Lehrbuch der Anorganischen Chemie*, Walter de Gruyter, Berlin, Germany, 101st edn, 1995.
- 20 F. O. Rice and C. J. Grelecki, *J. Am. Chem. Soc.*, 1957, **79**(11), 2679–2680.
- 21 R. A. Rowe and L. F. Audrieth, *J. Am. Chem. Soc.*, 1956, **78**(3), 563–564.
- 22 H. H. Sisler, M. A. Mathur, S. R. Jain and R. Greengard, *Ind. Eng. Chem. Prod. Res. Dev.*, 1981, **20**, 181–185.
- 23 L. J. Madginski, K. S. Pillay, H. Richard and Y. L. Chow, *Can. J. Chem.*, 1978, **56**, 1657–1667 and references therein.
- 24 W. McBride and H. W. Kruse, *J. Am. Chem. Soc.*, 1957, **79**(3), 572–577.
- 25 W. H. Urry, P. Szecsi and D. W. Moore, *J. Am. Chem. Soc.*, 1964, **86**(11), 2224–2229.
- 26 S. N. Singh and R. K. Prasad, *J. Indian Chem. Soc.*, 1992, **69**(10), 648–650.
- 27 W. R. McBride and H. W. Kruse, *US Pat.*, 3 135 800, 1952.
- 28 Method A: hold temperature at 90 °C for 1 min, then heat at 2 °C min⁻¹ to 130 °C.
- 29 (a) T. M. Klapötke and C. Miró Sabaté, *Z. Anorg. Allg. Chem.*, 2008, **634**, 1017–1024; (b) T. M. Klapötke and C. Miró Sabaté, *Eur. J. Inorg. Chem.*, 2008, 5350–5366.
- 30 (a) K. Karaghiosoff, T. M. Klapötke, P. Mayer, C. Miró Sabaté, A. Penger and J. M. Welch, *Inorg. Chem.*, 2008, **47**, 1007–1019; (b) C. Darwich, T. M. Klapötke and C. Miró Sabaté, *Chem.-Eur. J.*, 2008, **14**, 5756–5771; (c) T. M. Klapötke, C. Miró Sabaté, A. Penger, M. Rusan and J. M. Welch, *Eur. J. Inorg. Chem.*, 2009, 880–896.
- 31 F. R. Benson, *The High Nitrogen Compounds*, Wiley, New York, 1984.
- 32 N. B. Colthup, L. H. Daly and S. E. Wiberley, *Introduction to Infrared and Raman Spectroscopy*, Academic Press, Boston, USA, 1990.
- 33 N–N and N=N bond lengths from: *International Tables for X-ray Crystallography*, Kluwer Academic Publishers, Dordrecht, 1992, vol. C.

- 34 T. M. Klapötke and C. Miró Sabaté, *Chem. Mater.*, 2008, **20**(5), 1750–1763; T. M. Klapötke and C. Miró Sabaté, *Chem. Mater.*, 2008, **20**(11), 3629–3637; T. M. Klapötke and C. Miró Sabaté, *New J. Chem.*, 2009, **33**, 1605–1617.
- 35 B. Kovacevic, Z. B. Maksic and P. Rademacher, *Chem. Phys. Lett.*, 1998, **293**, 245–250.
- 36 G. S. Hammond, B. Seidel and R. E. Pincock, *J. Org. Chem.*, 1963, **28**, 3275–3279.
- 37 M. D. Walkinshaw, *Acta Crystallogr., Sect. C: Cryst. Struct. Commun.*, 1986, **42**, 246–249.
- 38 *CrysAlis CCD*, Version 1.171.27p5 beta; Oxford Diffraction Ltd.
- 39 *CrysAlis RED*, Version 1.171.27p5 beta; Oxford Diffraction Ltd.
- 40 SIR-92, A program for crystal structure solution: A. Altomare, G. Cascarano, C. Giacovazzo and A. Guagliardi, *J. Appl. Crystallogr.*, 1993, **26**, 343; G. M. Sheldrick, *SHELXS-97, Program for Crystal Structure Solution*, University of Göttingen, Germany, 1994; G. M. Sheldrick, *SHELXS-97, Program for Crystal Structure Solution*, University of Göttingen, Germany, 1997.
- 41 L. J. Farrugia, *J. Appl. Crystallogr.*, 1999, **32**, 837.
- 42 SCALE3 ABSPACK—An Oxford Diffraction program, Oxford Diffraction Ltd., 2005.
- 43 Crystal structure solution and refinement: formula = $C_8H_{10}N_4O_7$, MW = 274.18 g mol⁻¹, $T = 100(2)$ K, cryst. syst. = orthorhombic, space gr. = $Pb2a$, $a = 9.989(1)$ Å, $b = 11.085(1)$ Å, $c = 21.314(1)$ Å, $V = 2360.1(4)$ Å³, $Z = 8$, $\rho = 1.544$ g cm⁻³, $\mu = 0.352$ cm⁻¹, $F(000) = 780$ e, θ range = 3.82–29.60°, hkl range = $-10 \leq h \leq 10$, $-9 \leq k \leq 9$ and $-11 \leq l \leq 11$, refl. meas. = 7345, refl. unique = 1378, $R_{int} = 0.033$, $R(F)/wR(F^2)$ (all refl.) = 0.0502/0.0937, GoF (F^2) = 0.9963.
- 44 M. C. Etter and J. C. MacDonald, *Acta Crystallogr., Sect. B: Struct. Sci.*, 1990, **46**, 256–262; J. Bernstein, R. E. Davis, L. Shimoni and N. L. Chang, *Angew. Chem.*, 1995, **107**, 1689–1708 (*Angew. Chem., Int. Ed. Engl.*, 1995, **34**, 1555).
- 45 <http://www.ccdc.cam.ac.uk/suport/documentation/rpluto/TOC.html>.
- 46 A. D. Becke, *J. Chem. Phys.*, 1993, **98**, 5648.
- 47 C. Lee, W. Yang and R. G. Parr, *Phys. Rev. B*, 1988, **37**, 785.
- 48 E. D. Glendening, A. E. Reed, J. E. Carpenter and F. Weinhold, *Gaussian 03, Revision, D.01*, Gaussian, Inc., Wallingford, CT, 2004.
- 49 A. P. Scott and L. Radom, *J. Phys. Chem.*, 1996, **100**, 16502.
- 50 W. H. Bruning, C. J. Michejda and D. Romains, *Chem. Commun.*, 1967, 11–12.